hydrology

MDPI

Article

Soil Water Balance and Shallow Aquifer Recharge in an Irrigated Pasture Field with Clay Soils in the Willamette Valley, Oregon, USA

Daniel G. Gómez [1,2], Carlos G. Ochoa [1,*], Derek Godwin [1,3], Abigail A. Tomasek [4] and María I. Zamora Re [3]

1 Ecohydrology Lab, College of Agricultural Sciences, Oregon State University, Corvallis, OR 97331, USA; gomezdan@oregonstate.edu (D.G.G.); derek.godwin@oregonstate.edu (D.G.)
2 Water Resources Graduate Program, Oregon State University, Corvallis, OR 97331, USA
3 Department of Biological and Ecological Engineering, Oregon State University, Corvallis, OR 97331, USA; maria.zamorare@oregonstate.edu
4 Department of Crop and Soil Science, Oregon State University, Corvallis, OR 97331, USA; abigail.tomasek@oregonstate.edu
* Correspondence: carlos.ochoa@oregonstate.edu

Abstract: Quantifying soil water budget components, and characterizing groundwater recharge from irrigation seepage, is important for effective water resources management. This is particularly true in agricultural fields overlying shallow aquifers, like those found in the Willamette Valley in western Oregon, USA. The objectives of this two-year study were to (1) determine deep percolation in an irrigated pasture field with clay soils, and (2) assess shallow aquifer recharge during the irrigation season. Soil water and groundwater levels were measured at four monitoring stations distributed across the experimental field. A water balance approach was used to quantify the portioning of different water budget components, including deep percolation. On average for the four monitoring stations, total irrigation applied was 249 mm in 2020 and 381 mm in 2021. Mean crop-evapotranspiration accounted for 18% of the total irrigation applied in 2020, and 26% in 2021. The fraction of deep percolation to irrigation was 28% in 2020 and 29% in 2021. The Water Table Fluctuation Method (WTFM) was used to calculate shallow aquifer recharge in response to deep percolation inputs. Mean aquifer recharge was 132 mm in 2020 and 290 mm in 2021. Antecedent soil water content was an important factor influencing deep percolation. Study results provided essential information to better understand the mechanisms of water transport through the vadose zone and into shallow aquifers in agricultural fields with fine-textured soils in the Pacific Northwest region in the USA.

Keywords: water balance; water table fluctuation method; irrigated pastures; deep percolation; aquifer recharge; clay soils

Citation: Gómez, D.G.; Ochoa, C.G.; Godwin, D.; Tomasek, A.A.; Zamora Re, M.I. Soil Water Balance and Shallow Aquifer Recharge in an Irrigated Pasture Field with Clay Soils in the Willamette Valley, Oregon, USA. *Hydrology* **2022**, *9*, 60. https://doi.org/10.3390/hydrology9040060

Academic Editors: Ilmoon Chung, Sunwoo Chang, Yeonsang Hwang and Yeonjoo Kim

Received: 9 March 2022
Accepted: 31 March 2022
Published: 4 April 2022

1. Introduction

Numerous investigations have demonstrated that irrigation can lead to deep percolation, and recharge shallow aquifers while also providing return flows to nearby streams [1–4]. Deep percolation is highly dependent on soil physical characteristics, extraction patterns of the roots, ponding time at the surface, and depth to the water table [5–7]. Clay soils are especially important because their high field capacity allows for more water storage while their lower transmissivity rates slow water percolation through the soil profile, thereby potentially increasing water lost to evapotranspiration [8,9]. By contrast, clay soils are sensitive to drying and wetting cycles that can create cracks in the soil profile and cause macropore flow paths that rapidly deliver water, nutrients, and pollutants down to the water table [10].

As the western USA continues to experience exceptional drought, it is imperative to understand the relationship between water use and transport. Greater understanding

of surface water–groundwater interactions (SW-GW) will be essential for farmers and water managers to better estimate field water budget components, recharge-to-irrigation ratios, and potential pollutant leaching (e.g., nitrogen), while improving overall water management decisions affecting irrigation water supply and return flows to surface water and groundwater reservoirs [11,12]. The water balance method (WBM) can be used to estimate deep percolation below the root zone when reliable field observations are available. In many studies, deep percolation has been associated with aquifer recharge estimates [5,13]. Groundwater recharge is commonly quantified using approaches such as the Water Table Fluctuation Method (WTFM) [13,14]. The WTFM is often used because water level data is relatively easy to measure, and the WTFM assumes that rises in the water table are caused by actual recharge [14,15]. The method relies on the specific yield of an aquifer, defined as "the volume of water released from a unit volume of saturated aquifer material drained by a falling water table," multiplied by changes in the water level [14]. Recharge estimates using the WTFM are based on the premise that observed groundwater-level rises are directly related to irrigation or precipitation recharge arriving to the water table [13,16]. The WFTM's limitations are, firstly, the difficulty in obtaining an accurate specific yield value for a particular aquifer and, secondly, that specific yield varies by depth [15,17].

The specific connections between SW-GW, as they relate to water transport through the vadose zone and into the shallow aquifer, have not been fully explored in pasturelands of the Willamette River Basin. In this investigation, soil physical properties (e.g., soil texture and bulk density) and soil water content were utilized to assess water movement through the vadose zone and into the shallow aquifer of an irrigated, livestock-grazed pastureland in the Willamette Valley in western Oregon, USA. Objectives of this two-year study were to (1) determine deep percolation in an irrigated pasture field with clay soils, and (2) assess shallow aquifer recharge during the irrigation season.

2. Materials and Methods

2.1. Site Description

This two-year (2020 and 2021) study was conducted in a 2.1 ha pasture field (44.568 Lat.; 123.301 Long.) at the Oregon State University (OSU) Dairy Center in Corvallis, Oregon, USA. The site is located in western Oregon, in the Willamette Valley. The pasture field drains south, and is bordered by a discharge channel to the west, gravel roads to the north and east, and Oak Creek to the south (Figure 1). The field is irrigated with water pumped from Oak Creek. Streamflow in the discharge channel is negligible during the summer. No groundwater pumping for agriculture exists in the area. Depending on streamflow and soil water conditions following winter precipitation, irrigation at the OSU Dairy Center typically starts in early summer. However, due to modifications conducted on the irrigation pipes at the stream pumping site, the onset of the 2020 irrigation was delayed several weeks. The irrigation seasons ran from 27 July to 12 September in 2020, and from 15 June to 9 September in 2021. Vegetation at the study site included a mixture of balansa clover (*Trifolium michelianum balansae*), subterranean clover (*Trifolium subterraneum*), white clover (*Trifolium repens*), perennial ryegrass (*Lolium perenne*), annual ryegrass (*Lolium multiflorum*), orchard grass (*Dactylis glomerata*), and common chicory (*Cichorium intybus*) that was used for dairy cattle grazing in late spring and summer. Two soils series, as described in the USDA official series description [18], were present at the study site: Bashaw clay covered 55.8% of the experimental field while Holcomb silt loam covered 44.2%. Both soil series show slope values of 0% to 3%. Average depth to water table ranges between 0 to 76 mm in the winter rainy season, while the drainage class falls within the 'somewhat-poorly-drained' category for the Bashaw Clay and 'poorly-drained' category for the Holcomb silt loam [18]. Depth to water table, measured at the lowest level at the onset of the 2020 irrigation season, ranged between 1.2 and 1.6 m. The region has a Mediterranean type of climate with a warm and dry season in the summer and a mild and wet winter season. Most precipitation occurs as rainfall between November and April. Mean annual precipitation in the basin ranges from 2500 mm at higher elevations to 1000 mm in the valley where our study site was

located. The monthly-averaged lowest temperature happens in January (0.67 °C), while the highest occurs in August (27.4 °C). The lowest and highest total monthly precipitations happen in July (9.1 mm) and December (181.4 mm), respectively, [19].

Figure 1. Study site illustrating the location of the four monitoring stations used to measure soil water content and groundwater levels. Study site (44.568 Lat.; −123.301 Long.) is in Benton County, Oregon, USA.

2.2. Field Data Collection

Multiple field-based water, soil, and weather data were used to determine soil properties, calculate the field water budget, and estimate shallow aquifer recharge during the two years of the experiment.

2.2.1. Soil Water Content and Soil Physical Properties

Four soil water stations (North, South, West, and East) were installed on the pasture field (see Figure 1). Each station included a vertical network of three soil volumetric water content (θ) sensors (Model CS455, Campbell Scientific Inc., Logan, UT, USA) installed at 0.2, 0.5, and 0.8 m depths. At each station, the sensors were connected to a CR300 datalogger (Campbell Scientific Inc., Logan, UT, USA) programed to hourly record θ data. Three soil samples were collected at each sensor depth for characterizing soil physical properties (i.e., dry bulk density (ρ_b) and texture). The samples were obtained using a split soil core sampler (50 mm × 100 mm) (AMS Inc., American Falls, ID, USA). Soil samples at 0.2 and 0.5 m depths were collected from 43 additional locations spaced every 25 m to create a grid covering the entire pasture field. All soil samples were analyzed for ρ_b, using the core method [20], and for soil texture, using the hydrometer method [21].

Ordinary Kriging (OK), a geospatial interpolation method using ArcGIS Pro (version 2.8; Redlands, CA, USA), was used to project clay content distribution across the entire pasture field at selected dates during the irrigation season. Clay content was chosen as the soil texture variable of interest due to its influence on water-holding capacity, and therefore in θ. The assumption, in using the OK method, was that statistical and spatial relationships among measured points exist, and value predictions in neighboring spaces are possible due to the existence of spatial correlations.

2.2.2. Irrigation

The pasture field was irrigated using a pod sprinkler system (K-Line North America© 2016). The K-Line irrigation system consisted of two lines of sprinkler pods extending from two irrigation pipe risers in the center of the field. One line had 9 sprinkler pods while the other had 8, and each line was rotated approximately every 24 h to cover the entire field in four days. After a 3-day resting period, a new 4-day irrigation cycle would begin. When the soil conditions were drier, the sprinklers were kept running for about 48 h before being moved to the next location within the field. For example, due to modifications conducted on the irrigation pipes at the pumping site in the creek, the onset of the 2020 irrigation was delayed by several weeks. As a result, initial soil conditions were much drier, and each subsection was initially irrigated for 48 h to raise soil moisture conditions to an adequate level. Four transects, consisting of metal and plastic containers (108 mm diameter), were used as water-collectors to measure the amount of water applied during each 24 or 48 h irrigation application. The water-collectors were placed at 1.5, 3, 4.5, 6, 7.5, and 9 m from the center of two sprinklers on each line. The location of the water-collector transects was rotated to different sprinklers throughout the season to capture potential water-application variability. An additional plastic gauge was installed at each soil water station to measure the amount of irrigation water reaching the sensors' location. Regardless of the irrigation application duration (24 vs. 48 h), all water-collectors were measured approximately every 24 h. In addition to the daily-measured irrigation applications, an in-flow meter (UltraMag; McCrometer Inc., Hemet, CA, USA) was installed in each of the two irrigation lines to measure total water application during the 2021 irrigation season.

2.2.3. Groundwater Level

Data from shallow monitoring wells were used to characterize irrigation season aquifer recharge during the two years evaluated. One well was installed next to each of the θ stations at approximately 5 m deep and consisted of 50 mm diameter PVC pipes with a 1.5 m screen section in the bottom. These wells were equipped with CTD-10 (Decagon Devices Inc., Pullman, WA, USA) water level sensors. All water level sensors were connected to the CR300 dataloggers in each location and were programmed to hourly record water level data. All wells were surveyed to determine soil-surface and water-table elevations.

2.3. Soil Water Balance Method (SWBM)

A soil water balance approach was used to calculate *DP*, defined as the water passing below the 0.8 m sensor depth:

$$DP = IRR + P - RO - DS - AET \quad (1)$$

where *DP* = deep percolation (mm); *IRR* = irrigation depth (mm); *P* = precipitation (mm); D*S* = change in soil water storage (mm); *RO* = field runoff (mm); and *AET* = actual evapotranspiration (mm). *DP* was calculated for each soil-monitoring station, following individual irrigation applications to the corresponding subsection being irrigated. *IRR* was obtained from the water-collector-measured irrigation applications. *P* was obtained from the weather station records; no quantifiable *RO* occurred during either irrigation season. D*S* was calculated for each sensor depth (0.2, 0.5, and 0.8 m) based on the θ difference between the onset of irrigation and 48 h after the end of irrigation. D*S* was then averaged across all three sensor depths to represent the entire 0.8 m profile. *AET* was calculated using the reference *ETo* for short grass estimated by the weather station and multiplied by crop coefficient (*Kc*) values (0.25 to 0.68) developed by the USDA Agriculture Research Service for pastures in the Columbia-Pacific Northwest Region [22]. All the individual SWBM results obtained for each irrigation application were aggregated each year to obtain an overall seasonal SWBM estimate. Figure 2 illustrates the soil water- and groundwater-level instrumentation, and the water budget components evaluated.

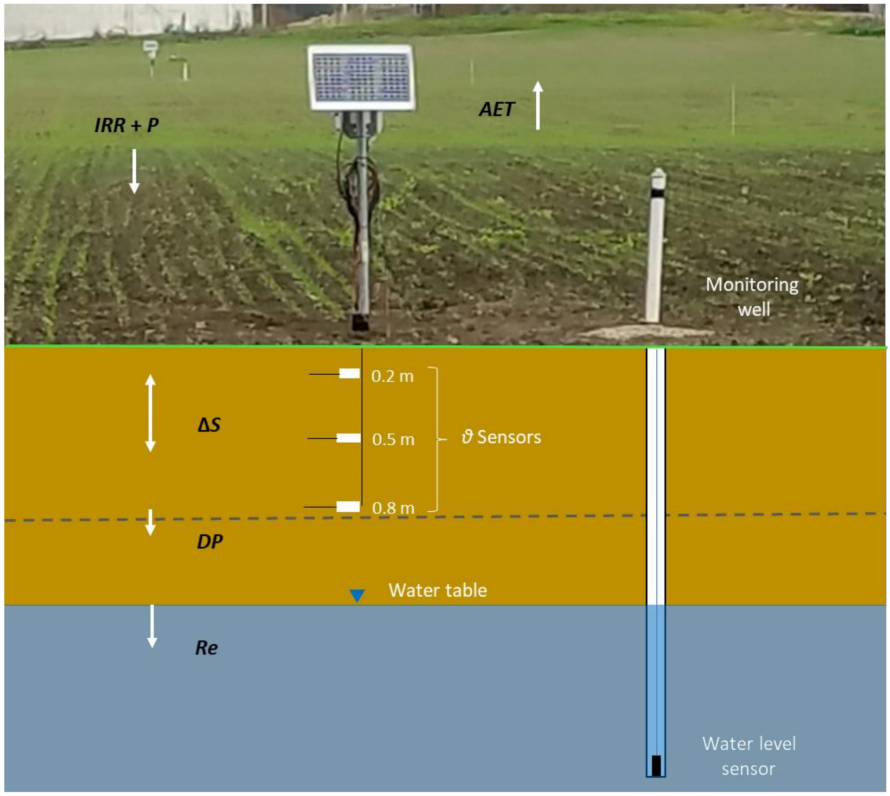

Figure 2. Schematic illustrating soil water (θ) and groundwater-levels measurement at each monitoring station. The main water budget components–irrigation (*IRR*), precipitation (*P*), change in soil water (Δ*S*), deep percolation (*DP*), actual evapotranspiration (*AET*), and aquifer recharge (*Re*)–are shown. Figure not to scale.

2.4. Shallow Aquifer Recharge

Groundwater-level fluctuations during the irrigation season were characterized using data from each monitoring well on the pasture field. The recharge (*Re,* in mm) of the shallow aquifer was calculated using the groundwater-level data from the wells in the pasture field, and the WTFM,

$$Re = \Delta h \times Sy \quad (2)$$

where *Re* = aquifer recharge (mm); Δ*h* = change in water level (mm); and *Sy* = specific yield of the unconfined aquifer. Data recorded by the water level sensors installed in the wells were used to determine changes in water level. As described in Sophocleous [14], dividing the potential recharge values (i.e., *DP*) by the associated rises in the water table over several events can provide a "site-calibrated effective storativity value". A mean *Sy* value of 0.06, with most values ranging from 0.03 to 0.06, was estimated based on the *DP* events observed during the two irrigation seasons. The exception was a *Sy* value of 0.13 obtained for the South well location in 2020. Our field based *Sy* values were similar to the *Sy* mean value of 0.06, and ranging from 0.01 to 0.18, for clay materials reported in Dingman [23].

2.5. Statistical Analyses

An Analysis of Variance (ANOVA) was performed to explore the relationships of seasonal aquifer recharge, *Re*, observed at each monitoring well in 2020 and 2021. For each soil-monitoring station, we also conducted a linear-regression analysis to test the relationship between total water applied (*TWA*) and *DP*. Our previous research [2,5] had shown that antecedent soil water can have a significant effect on deep percolation. Therefore, we also ran the linear-regression analysis, subtracting Δ*S* from *TWA*. SigmaPlot® version 14.0 (Systat Software Inc., San Jose, CA, USA) was used for all the statistical analyses.

3. Results

3.1. Soil Properties

Soil texture and ρ_b varied across soil water stations and sensor depths (Table A1). Finer-texture soils were found in the East and West stations in the middle of the field. Clay loam soils were found for all sensor depths at the top (North station) and at 0.5 and 0.8 m depths at the bottom (South station) of the field. Coarser (54% sand) texture was observed at 0.2 m depth in the South station, which also had the lowest ρ_b values.

Field-scale clay content distribution analysis showed the highest clay content in the middle of the field (Figure 3). This was the case for the 0.5 m depth, with values ranging from 32% to 35% near the North station and from 35% to 38% near the South station (Figure 3b). In addition, higher clay content values (38% to 41%) were estimated for areas near the stations in the middle of the field, which were consistent with the 43% and 45% values obtained for the East and West stations. More discrepancy was observed at the 0.2 m depth. Although higher than the clay content values at the top and bottom of the field, the highest values of 32% to 35% observed in the middle of the field were below the 43% and 45% values obtained at the East and West stations, respectively, (Figure 3a; Table A1).

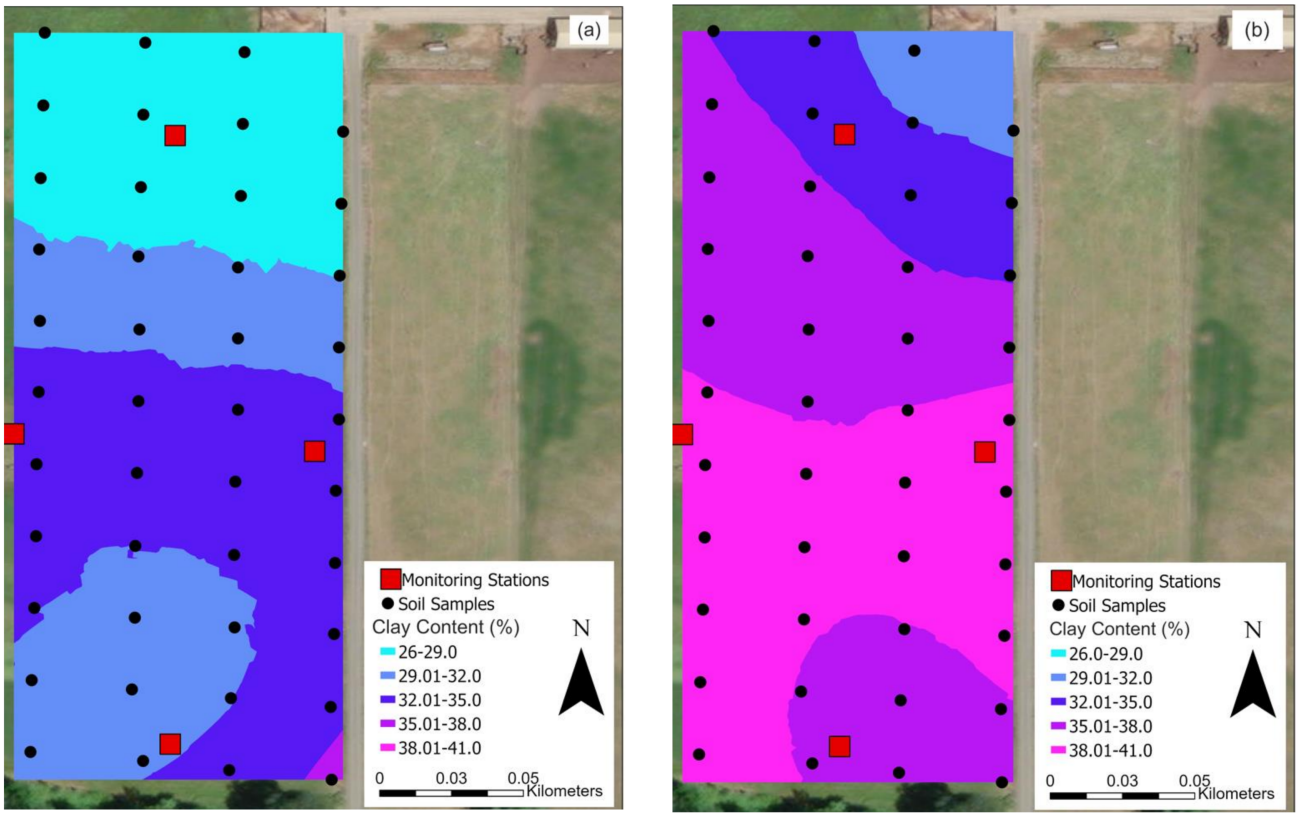

Figure 3. Clay distribution using data from the 43 soil samples and monitoring stations using Ordinary Kriging at the (**a**) 0.2 m depth and (**b**) 0.5 m depth.

3.2. Soil Water Balance

DP was variable among stations and irrigation seasons (Table 1). At the end of the 2020 season, the South station had the largest amount of cumulative *DP* (98 mm), followed by the West (94 mm), East (69 mm), and North (20 mm) stations (Table 1). The amount of *DP* for each station did not appear to be related to the cumulative amount of *TWA* (*IRR* + *P*), as the East station had the largest total *IRR* (280 mm) for 2020 but resulted in the second lowest total *DP* amount (69 mm). In comparison, the West station *IRR* was 214 mm (the smallest of the season) resulting in 94 mm of *DP* (the second largest). For the 2021 irrigation period, the most groundwater recharge through *DP* occurred in the West station (153 mm), followed

by the East (101 mm), South (99 mm), and North station (92 mm). The greatest amount of *TWA* during this season corresponded to the South station (391 mm), which had the second lowest amount of *DP* (99 mm). By comparison, the North station *TWA* was 368 mm (smallest of the season), and resulted in 92 mm of *DP*, the lowest of the season. Total *DP* across all stations in 2020 was 281 mm, and *TWA* was 1,006 mm, while in the longer 2021 season, *DP* was 445 mm with a *TWA* of 1,524 mm (Table 1). The statistical analysis showed that the relationships between *DP* and *TWA* alone were weak ($p > 0.05$) for all stations during both irrigation seasons. However, the role of antecedent soil water, as reflected in ΔS, was an important factor in estimating *DP*. The regression analysis conducted for all irrigation applications in each year showed a positive linear relationship ($p \leq 0.05$; R^2 values from 0.72 to 0.99) between *DP* and *TWA* - ΔS for all soil stations in 2020, but not for the East station in 2021. Overall, seasonal *TWA* values were higher than ΔS, with the fraction of ΔS to *TWA* ranging from 0.4% to 0.8%. The exception was the North station in 2020 when ΔS exceeded *TWA*. The monitoring station was toward the bottom of a more pronounced slope in that part of the field. We believe that potential oversaturation of the soil profile at this station may have occurred during the longer 48 h irrigation events used to raise soil water conditions at the beginning of the 2020 season.

Table 1. Water budget component results for each soil monitoring station (North, West, East, and South) during the 2020 and 2021 irrigation seasons. The water budget components are irrigation (*IRR*), precipitation (*P*), total change in soil water (ΔS), evapotranspiration (*AET*), and deep percolation (*DP*). The season-cumulative results for all irrigation applications (n) for each station are shown. All results are reported in mm.

Year	Station	n	*IR*	*P*	*DS*	*AET*	*DP*
2020	North	6	250	9	302	42	20
	West	6	214	9	114	45	94
	East	6	280	9	238	52	69
	South	6	253	9	118	45	98
2021	North	13	368	0	202	96	92
	West	13	386	0	150	99	153
	East	13	379	0	233	95	101
	South	13	391	0	285	99	99

3.3. Groundwater Levels and Aquifer Recharge

A gradual rise in groundwater levels, following the onset of the irrigation season, was observed in all four wells during both years. Overall, groundwater levels remained higher (up to 1.2 m) than initial conditions through both irrigation seasons. Groundwater levels in all wells rose from the beginning to the end of the 2020 irrigation season, while in 2021 the North and East wells' groundwater levels rose throughout the summer (Figure 4a,b). A relatively moderate rise and decline in groundwater levels was observed after all six irrigation applications at each well location in 2020. The exception was the North well, following the first irrigation (Figure 4). The more frequent and larger number (n = 13) of irrigation applications in 2021 resulted in relatively sharp groundwater level rises and declines in all wells. The South well appeared to show groundwater level increases even when no direct on-site water applications occurred. This was attributed to the location of the well at the bottom of the pasture, which may have been affected by lateral flow contributions from the irrigation in other parts of the field. The groundwater level rises observed in the West well illustrate the saturated-ponding conditions that occurred during several irrigation events in 2021 when peak water-level-rise plateaued for several hours before receding. During the 2020 irrigation season, groundwater levels in the West well showed a diurnal oscillation that was attributed to water uptake from the riparian vegetation present in a storm discharge channel adjacent to the experimental pasture field. Heavier clay content conditions and a lower terrain were observed at this West well location.

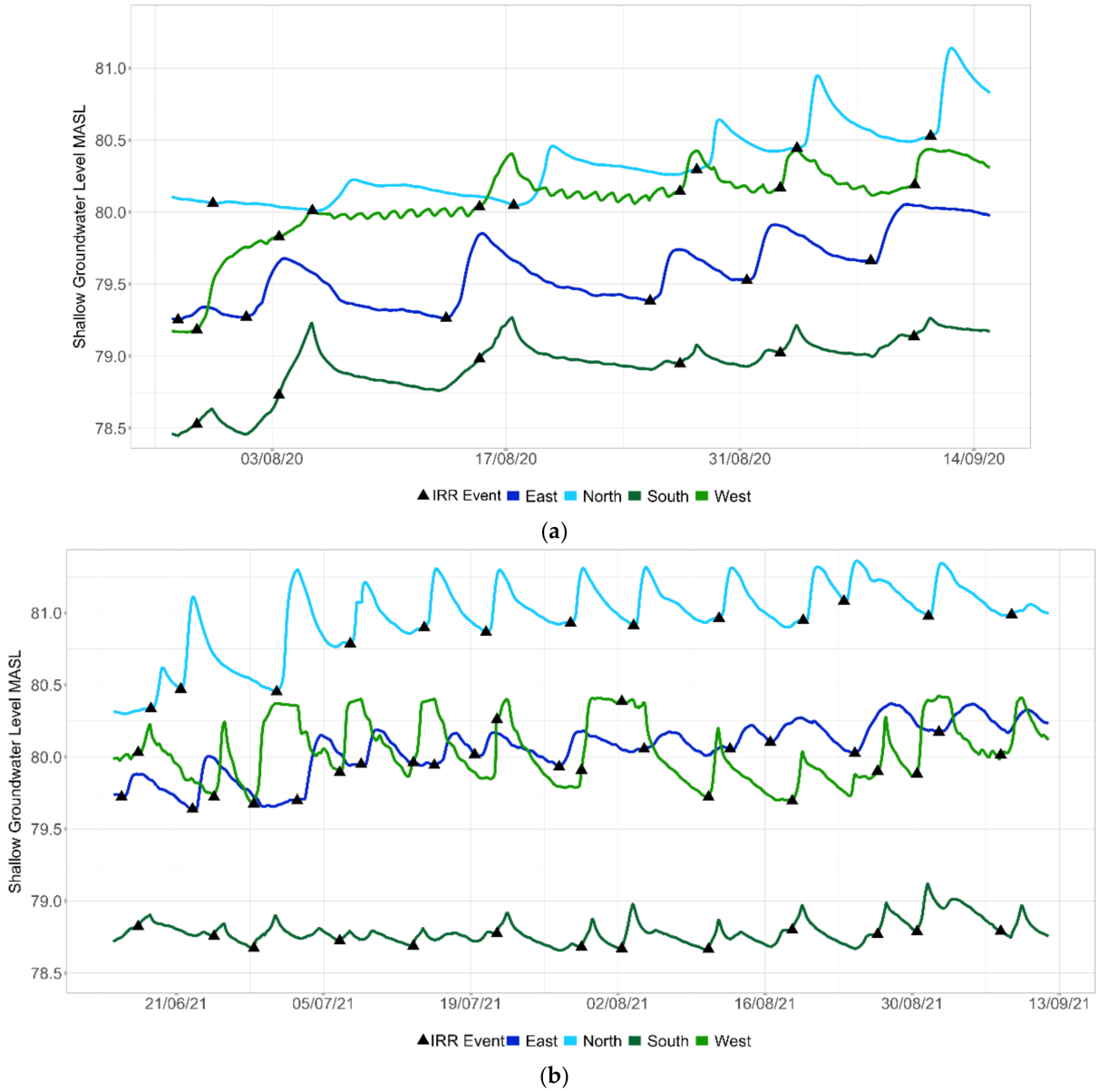

Figure 4. Daily averaged groundwater level in meters-above-sea-level (MASL) at the four monitoring wells on the experimental field during the (**a**) 2020 and (**b**) 2021 irrigation seasons. The irrigation events (*IRR*) for the area near each well location are also illustrated.

The substantially fewer number of *IRR* events at each soil station in 2020 (mean of 449 mm) compared to 2021 (mean of 568 mm) was reflected in the lower *Re* values obtained for each well location. On average, total seasonal aquifer recharge was 132 mm in 2020 and 290 mm in 2021. The *Re* estimates for each monitoring well were less variable in 2020 than in 2021 (Table 2). In 2020, total *Re* ranged from 128 mm in the North well to 137 mm in the East and West wells. In 2021, total *Re* ranged from 190 mm in the West well to 352 mm in the East well. The ANOVA results showed that mean seasonal *Re* was not significantly different ($p > 0.05$) among all four wells in 2020. However, a Kruskal–Wallis One-Way ANOVA on Ranks showed seasonal *Re* was significantly different ($p \leq 0.05$) for West vs. South and North vs. South wells.

Table 2. Irrigation season total groundwater recharge (*Re*) and total irrigation (*IRR*) for each monitoring well location. All measurements are reported in mm.

	2020		2021	
Station	***Re***	***IRR***	***Re***	***IRR***
North	128	358	340	438
East	137	526	352	460
West	137	385	190	628
South	130	528	278	745

4. Discussion

This investigation explored the connections between surface water and shallow groundwater as they relate to irrigation water transport through the vadose zone into the shallow aquifer. Study results indicated that soil physical attributes observed across the field played an important role in *DP* and aquifer response. A relatively shallow aquifer (<2 m) and preferential flow may have contributed to the rapid transport of irrigation water through the soil profile and into the shallow aquifer. Similar to that reported in other studies [2,24], irrigation frequency and antecedent soil water content were important variables affecting *DP* and shallow aquifer recharge. Differences in the *TWA* and frequency of irrigation were important for the greater *DP* and shallow aquifer recharge estimates observed at the end of the irrigation season in the second year of the experiment. The higher frequency of irrigation events observed during the 2021 irrigation season helped maintain higher soil-moisture levels and, consequently, more *DP* and aquifer recharge than in the previous year. Irrigation frequency and irrigation duration differences between the two seasons likely impacted *DP* distinctly, as research has shown that even an hour's break in irrigation causes the upper part of the soil profile to desaturate and allows for air to enter the soil profile and to fill pores, disrupting *DP* [25]. At the beginning of both seasons, *TWA* was slow to saturate the soil, with most of the water stored in the soil profile, and consequently less *DP* was observed. Antecedent soil water content was important in the *DP* estimates obtained for individual irrigation events. The change in soil water content (ΔS) made up 47% to 85% of total irrigation in 2020, and 39% to 73% in 2021. The effects of *TWA* for individual irrigation events were less apparent, and no strong relationships between irrigation amount and *DP* were obtained. This was partly attributed to the relatively low amounts of water applied (mean = 29 mm) during each irrigation event. At the beginning of both irrigation seasons, groundwater level rises occurred before the soil sensors' profile (upper 0.8 m) reported saturation.

Overall, cumulative *Re* estimates during both irrigation seasons were greater than *DP*. This is different from the results of a previous study [5] conducted in flood-irrigated fields with highly permeable soils in the southwestern USA. The larger *Re* estimates obtained in this study were attributed to irrigation water moving down the soil profile to the shallow aquifer through macropore flow paths, which is a behavior that has been documented in other deep percolation investigations (e.g., [24,26]). We credited the potential presence of macropore flow paths to the soil physical properties of the experimental field. A study conducted by [27] in a field near our study site revealed the presence of macropore flow due to shrinking and swelling of the clayey soil, paths caused by earth worms, and tunnels dug by voles. The transient water-contributions to the shallow aquifer from recently applied irrigations in neighboring sections of the field may have resulted in the larger *Re* values observed when compared to the *DP* values based on soil water estimates. The large differences in *Re* vs. *DP* obtained using different techniques (SWBM vs. WTFM) indicate caution ought to be exercised when assessing irrigation contributions to the shallow groundwater system.

The potential presence of preferential flow paths could also help explain the difference in *DP* and *Re* calculations between the stations during both seasons. For example, both the West (40.6%) and East (43.8%) stations had the highest average clay content but never had the lowest *DP* or *Re* calculations. The higher clay content may have resulted in a

higher number of preferential pathways available for water to rapidly reach the shallow aquifer [9] while minimizing the amount of water lost to *ET* and stored in the soil profile. Rapid responses from the water table were observed throughout the season even when the soil reached saturation and cracks were no longer visible in the soil surface, which has been shown to stop preferential flow due to soil swelling [28]. However, previous research [29] has shown that sprinkler irrigation may only partially close soil cracks, maintaining an avenue for rapid water transport. Preferential flow paths may also persist in the deeper levels of a saturated soil subsurface [30] while others may only partially close or remain fully open throughout the soil profile [31]. The presence of preferential flow paths could be determined using lab [32] or field [33] dye experiments. The existence and role of preferential flow paths in soil water and groundwater recharge at this experimental pasture field remain unknown: further investigation may be needed to determine if that is a condition that can help explain the shallow groundwater-level fluctuations and *Re* values obtained in this study.

Study limitations included a later start in the 2020 irrigation season than in 2021. This caused adjustments in the irrigation scheduling during the first year (a smaller number of irrigation events, longer duration) to compensate for the drier soil conditions observed at the beginning of the season. In addition, the type of rotational irrigation system (pod sprinkler) employed did not allow for full irrigation cover across the entire field at the same time. The field was separated in four subsections, and *DP* and *Re* estimated for each individual subsection. Therefore, no direct comparison of specific *DP* events and *Re* was conducted. Instead, we calculated *Re* based on the various distinct water table rises and declines observed during each irrigation season. The soil water content sensors used in this study were not calibrated for site-specific soil characteristics. It is possible that some of the SWBM calculations (i.e., ΔS) may have been affected by potential discrepancies in θ readings.

Beyond improved measurements for the water balance and aquifer recharge methodology employed, results from this investigation contribute towards understanding of the relationships between irrigation, soil water, and shallow aquifer recharge in agricultural fields with fine-textured soils in the Pacific Northwest region of the USA. These findings can be used to aide water managers and farmers in similar agroecological systems, in determining the effect of irrigation on solute transport, groundwater recharge, and possibly streamflow augmentation during critical baseflow periods.

Author Contributions: C.G.O., D.G.G. and D.G. developed the study design and conducted field data collection. All authors contributed to data analyses and the writing of the manuscript. All authors have read and agreed to the published version of the manuscript.

Funding: This research received no external funding.

Institutional Review Board Statement: Not applicable.

Informed Consent Statement: Not applicable.

Acknowledgments: The authors gratefully acknowledge the various graduate and undergraduate students from Oregon State University who helped with field data collection activities related to the results presented here. The study was supported by the Oregon Agricultural Experiment Station.

Conflicts of Interest: The authors declare no conflict of interest.

Appendix A Soil Physical Properties and Textural Classification

Table A1. Soil physical properties by monitoring station: by depth, including mean values and standard error of the three samples collected at each depth to determine dry soil bulk density (ρ_b); soil particle distribution of sand, silt, and clay; and soil texture. Soil particle distribution was calculated using an aggregate of the three samples collected at each depth.

Station	Soil Depth (m)	ρ_b (Mg m^{-3})	Clay (%)	Silt (%)	Sand (%)	Soil Texture
North	0.2	1.5 ± 0.01	30.1	45.9	24.0	clay loam
	0.5	1.5 ± 0.01	30.7	39.9	29.3	clay loam
	0.8	1.4 ± 0.004	36.1	19.3	44.7	clay loam
West	0.2	1.5 ± 0.04	44.9	30.5	24.7	clay
	0.5	1.4 ± 0.02	43.5	43.1	13.3	silty clay
	0.8	1.6 ± 0.01	33.5	57.1	9.3	silty clay loam
East	0.2	1.7 ± 0.06	42.9	35.8	21.3	clay
	0.5	1.7 ± 0.04	44.2	32.5	23.3	clay
	0.8	1.6 ± 0.03	44.2	34.5	21.3	clay
South	0.2	1.0 ± 0.01	21.4	24.6	54.0	sandy clay loam
	0.5	1.1 ± 0.01	34.1	26.6	39.3	clay loam
	0.8	1.2 ± 0.02	39.4	23.3	37.3	clay loam

References

1. Arnold, L.R. *Estimates of Deep-Percolation Return Flow beneath a Flood- and a Sprinkler-Irrigated Site in Weld County, Colorado, 2008–2009*; U.S. Geological Survey Scientific Investigations Report 2011–5001; US Geological Survey: Reston, VA, USA, 2011; 225p.
2. Gutiérrez-Jurado, K.Y.; Fernald, A.G.; Guldan, S.J.; Ochoa, C.G. Surface water and groundwater interactions in traditionally irrigated fields in Northern New Mexico, U.S.A. *Water* **2017**, *9*, 102. [CrossRef]
3. Li, D. Quantifying water use and groundwater recharge under flood irrigation in an arid oasis of northwestern China. *Agric. Water Manag.* **2020**, *240*, 106326. [CrossRef]
4. Fernald, A.G.; Cevik, S.Y.; Ochoa, C.G.; Tidwell, V.C.; King, J.P.; Guldan, S.J. River Hydrograph Retransmission Functions of Irrigated Valley Surface Water–Groundwater Interactions. *J. Irrig. Drain. Eng.* **2010**, *136*, 823–835. [CrossRef]
5. Ochoa, C.G.; Fernald, A.G.; Guldan, S.J.; Tidwell, V.C.; Shukla, M.K. Shallow Aquifer Recharge from Irrigation in a Semiarid Agricultural Valley in New Mexico. *J. Hydrol. Eng.* **2013**, *18*, 1219–1230. [CrossRef]
6. Bethune, M.G.; Selle, B.; Wang, Q.J. Understanding and predicting deep percolation under surface irrigation. *Water Resour. Res.* **2008**, *44*, 1–16. [CrossRef]
7. Bethune, M. Towards effective control of deep drainage under border-check irrigated pasture in the Murray-Darling Basin: A review. *Aust. J. Agric. Res.* **2004**, *55*, 485–494. [CrossRef]
8. Lal, R.; Shukla, M.K. *Principles of Soil Physics*; Marcel Dekker: New York, NY, USA, 2004.
9. Baram, S.; Kurtzman, D.; Dahan, O. Water percolation through a clayey vadose zone. *J. Hydrol.* **2012**, *424–425*, 165–171. [CrossRef]
10. Kurtzman, D.; Scanlon, B.R. Groundwater Recharge through Vertisols: Irrigated Cropland vs. Natural Land, Israel. *Vadose Zone J.* **2011**, *10*, 662–674. [CrossRef]
11. Boyko, K.; Fernald, A.G.; Bawazir, A.S. Improving groundwater recharge estimates in alfalfa fields of New Mexico with actual evapotranspiration measurements. *Agric. Water Manag.* **2021**, *244*, 106532. [CrossRef]
12. Grogan, D.S.; Wisser, D.; Prusevich, A.; Lammers, R.B.; Frolking, S. The use and re-use of unsustainable groundwater for irrigation: A global budget. *Environ. Res. Lett.* **2017**, *12*, 034017. [CrossRef]
13. Scanlon, B.R.; Healy, R.W.; Cook, P.G. Choosing appropriate techniques for quantifying groundwater recharge. *Hydrogeol. J.* **2002**, *10*, 18–39. [CrossRef]
14. Sophocleous, M.A. Combining the soil water balance and water-level fluctuation methods to estimate natural groundwater recharge: Practical aspects. *J. Hydrol.* **1991**, *124*, 229–241. [CrossRef]
15. Healy, R.W.; Cook, P.G. Using groundwater levels to estimate recharge. *Hydrogeol. J.* **2002**, *10*, 91–109. [CrossRef]
16. Nimmer, M.; Thompson, A.; Misra, D. Modeling Water Table Mounding and Contaminant Transport beneath Storm-Water Infiltration Basins. *J. Hydrol. Eng.* **2010**, *15*, 963–973. [CrossRef]
17. Childs, E.C. The nonsteady state of the water table in drained land. *J. Geophys. Res.* **1960**, *65*, 780–782. [CrossRef]
18. Soil Survey Staff, Natural Resources Conservation Service, United States Department of Agriculture. Soil Series Classification Database. Available online: http://websurvey.sc.egov.usda.gov/ (accessed on 6 February 2021).

19. Oregon State University, Corvallis, Oregon, USA—Climate Summary. Available online: https://wrcc.dri.edu/cgibin/cliMAIN.pl?or1862 (accessed on 31 January 2022).
20. Blake, G.R.; Hartge, K.H. Bulk density. In *Methods of Soil Analysis, Part 1—Physical and Mineralogical Methods*; Agronomy Monographs 9; American Society of Agronomy: Madison, WI, USA, 1986; Volume 9.
21. Gee, G.W.; Bauder, J.W. Particle size analysis. In *Method of Soil Analysis, Part 1: Physical and Mineralogical Methods*; Klute, A., Ed.; Soil Science Society of America: Madison, WI, USA, 1986.
22. Bureau of Reclamation. Available online: https://www.usbr.gov/pn/agrimet/cropcurves/PASTcc.html (accessed on 12 January 2022).
23. Dingman, S.L. Ground water in the hydrologic cycle. In *Physical Hydrology*, 2nd ed.; Prentice Hall: Upper Saddle River, NJ, USA, 2002; pp. 325–388.
24. Ochoa, C.G.; Fernald, A.G.; Guldan, S.J.; Shukla, M.K. Deep percolation and its effects on shallow groundwater level rise following flood irrigation. *Trans. ASABE* **2007**, *50*, 73–81. [CrossRef]
25. Wangemann, S.G.; Kohl, R.A.; Molumeli, P.A. Infiltration and percolation influenced by antecedent soil water content and air entrapment. *Trans. ASAE* **2000**, *43*, 1517–1523. [CrossRef]
26. Ochoa, C.G.; Fernald, A.G.; Guldan, S.J.; Shukla, M.K. Water Movement through a Shallow Vadose Zone: A Field Irrigation Experiment. *Vadose Zone J.* **2009**, *8*, 414–425. [CrossRef]
27. Cassidy, J.R. Effect of Burrowing Mammals on the Hydrology of a Drained Riparian Ecosystem. Ph.D. Thesis, Oregon State University, Corvallis, OR, USA, 2002.
28. Römkens, M.J.M.; Prasad, S.N. Rain Infiltration into swelling/shrinking/cracking soils. *Agric. Water Manag.* **2006**, *86*, 196–205. [CrossRef]
29. Qi, W.; Zhang, Z.-y.; Wang, C.; Chen, Y.; Zhang, Z.-m. Crack closure and flow regimes in cracked clay loam subjected to different irrigation methods. *Geoderma* **2020**, *358*, 113978. [CrossRef]
30. Greve, A.K.; Acworth, R.I.; Kelly, B.F.J. Detection of subsurface soil cracks by vertical anisotropy profiles of apparent electrical resistivity. *Geophysics* **2010**, *75*, WA85–WA93. [CrossRef]
31. Greve, A.K.; Andersen, M.S.; Acworth, R.I. Monitoring the transition from preferential to matrix flow in cracking clay soil through changes in electrical anisotropy. *Geoderma* **2012**, *179–180*, 46–52. [CrossRef]
32. Zhang, Y.; Cao, Z.; Hou, F.; Cheng, J. Characterizing preferential flow paths in texturally similar soils under different land uses by combining drainage and dye-staining methods. *Water* **2021**, *13*, 219. [CrossRef]
33. Liu, M.; Guo, L.; Yi, J.; Lin, H.; Lou, S.; Zhang, H.; Li, T. Characterising preferential flow and its interaction with the soil matrix using dye tracing in the Three Gorges Reservoir Area of China. *Soil Res.* **2018**, *56*, 588–600. [CrossRef]